Emergent Magnetic Degeneracy in Iron Pnictides due to the Interplay between Spin-Orbit Coupling and Quantum Fluctuations

Morten H. Christensen,[1] Peter P. Orth,[2,3] Brian M. Andersen,[4] and Rafael M. Fernandes[1]
[1]School of Physics and Astronomy, University of Minnesota, Minneapolis, Minnesota 55455, USA
[2]Department of Physics and Astronomy, Iowa State University, Ames, Iowa 50011, USA
[3]Ames Laboratory, U.S. DOE, Iowa State University, Ames, Iowa 50011, USA
[4]Niels Bohr Institute, University of Copenhagen, Juliane Maries Vej 30, DK-2100, Denmark

(Received 20 December 2017; published 30 July 2018)

Recent experiments in iron pnictide superconductors reveal that, as the putative magnetic quantum critical point is approached, different types of magnetic order coexist over a narrow region of the phase diagram. Although these magnetic configurations share the same wave vectors, they break distinct symmetries of the lattice. Importantly, the highest superconducting transition temperature takes place close to this proliferation of near-degenerate magnetic states. In this Letter, we employ a renormalization group calculation to show that such a behavior naturally arises due to the effects of spin-orbit coupling on the quantum magnetic fluctuations. Formally, the enhanced magnetic degeneracy near the quantum critical point is manifested as a stable Gaussian fixed point with a large basin of attraction. Implications of our findings to the superconductivity of the iron pnictides are also discussed.

DOI: 10.1103/PhysRevLett.121.057001

Introduction.—Magnetism in the iron pnictide superconductors remains an intensely studied subject, not least due to its impact on unconventional superconductivity [1–3], but also as a playground for exploring unusual types of magnetic orders [4–6]. While early experiments reported the prevalence of a stripe spin-density wave (SSDW) in the phase diagrams of these systems [7,8], a series of recent experiments in several different compounds found a richer behavior [9–24]. As optimal doping is approached, the SSDW transition temperature is suppressed to zero, signaling a putative magnetic quantum critical point (QCP). In this region, other types of magnetic orders proliferate. Although these are characterized by the same wave vectors as the SSDW phase, $\mathbf{Q}_{1,2} = (\pi, 0), (0, \pi)$, they do not break the tetragonal symmetry of the lattice—hence being dubbed C_4 magnetic phases [12]. The proximity of the superconducting dome to this peculiar regime of intertwined magnetic phases with comparable transition temperatures raises important questions about the interplay between magnetism, quantum fluctuations, and superconductivity. Phenomenologically, these C_4 phases can be understood as double-$\mathbf{Q}$ configurations corresponding to a collinear or coplanar equal-weight superposition of $(\pi, 0)$ and $(0, \pi)$ orders—in contrast to the single-$\mathbf{Q}$ SSDW phase, which breaks tetragonal symmetry and is thus called the C_2 phase [6].

Several microscopic mechanisms have been proposed to explain their origin [4,5,25–35]. However, they generally suffer from two drawbacks. (i) The determination of the ground state follows from a mean-field analysis, which is unlikely to be valid near the putative QCP due to fluctuation effects. (ii) The system is assumed isotropic in spin space. The latter is in contradiction with the sizable spin-orbit coupling (SOC) observed in these systems [36], whose 100 K energy scale is comparable to the typical magnetic transition temperature. As a result, the spin anisotropies induced by SOC [29], which are experimentally observed by neutron scattering and NMR [37–44], cannot be neglected near the magnetic transition. More broadly, it is difficult to attribute the observed near degeneracy between the C_2 and C_4 phases only to material-specific properties, since this behavior is often seen close to the putative quantum critical point [see schematic Fig. 1(b)] and in several different unrelated compounds, such as hole-doped $BaFe_2As_2$ [12–15], pressurized FeSe [45], and electron-doped $CaKFe_4As_4$ [11].

In this Letter, we argue that this behavior is not a result of fine-tuned interactions, but instead is a universal property of the magnetism of the iron pnictides, provided that SOC and fluctuations are taken into account. Although this result is complementary to previous works on this topic, it provides a significant departure from the interpretation that the C_2-C_4 magnetic degeneracy arises solely from band structure effects. Universal properties are naturally described in terms of the renormalization-group (RG) approach, which we employ throughout this Letter. The RG flow describes how the system's mean-field parameters are renormalized by fluctuations. This allows us to assess the ground states and the character of the corresponding phase transitions.

The main results of our RG analysis near the putative magnetic QCP are shown schematically in Fig. 1(a). For the isotropic system (horizontal line), the RG flow pushes the system deep into either the C_2 or the C_4 phase. Moreover,

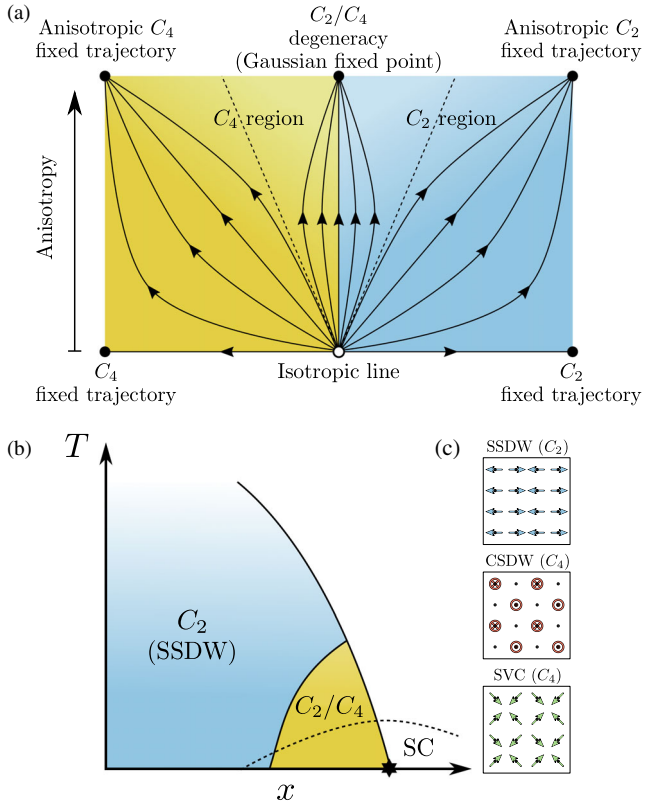

FIG. 1. (a) Schematics of our RG results. The arrows show how fluctuations affect the coefficients of the free energy, moving them away from their mean-field values derived from a microscopic band structure calculation. In the spin-isotropic case, fluctuations bring the system deep into either the C_2 or a C_4 phase, removing any fine-tuned degeneracy from the system that may exist at a mean-field level. When spin anisotropies are included, a new fixed point emerges in which the C_2 and C_4 phases are degenerate. Systems whose mean-field parameters lie within the fan of dashed lines are pushed to this fixed point by fluctuations. (b) Schematic phase diagram based on our renormalization-group calculations. Here, T is temperature and x is an external tuning parameter, such as doping or pressure. As the putative quantum critical point (QCP, denoted by a star) is approached, the interplay between spin anisotropy (driven by the spin-orbit coupling) and quantum fluctuations leads to a near degeneracy between the C_2 and C_4 magnetic phases. While the C_2 phase is always the stripe-spin density-wave (SSDW) state, the C_4 phase can be either the spin-vortex crystal (SVC) or the charge-spin density-wave (CSDW) state depending on whether the spin anisotropies force the moments in the plane or out of the plane, respectively, see (c).

the magnetic transition becomes first-order, indicating the absence of quantum critical fluctuations. Thus, even if the mean-field parameters (obtained, e.g., from band structure calculations) place the system close to the degeneracy between the C_2 and C_4 phases, fluctuations strongly remove this degeneracy. On the other hand, upon including the spin anisotropy promoted by the SOC (vertical line), a new fixed point in the RG flow emerges, in which the C_2 and C_4 magnetic phases are degenerate. Importantly, when the mean-field parameters are within the basin of attraction of this fixed point [indicated by the region between the dashed lines in Fig. 1(a)], the fluctuations will drive the system to the C_2-C_4 degenerate point. Indeed, the mean-field results of, e.g., Refs. [30,31] lie within this region. Thus, our main point is that the experimentally observed proliferation of nearly degenerate C_2 and C_4 magnetic phases in the iron pnictides is not a result of fine-tuning, but an emergent universal property of the magnetism of these systems. In the remainder of the Letter, we derive these results and discuss their implications for the superconducting state of the pnictides.

Renormalization group flow of the isotropic case.—Magnetic order in the iron pnictides is characterized by two distinct ordering wave vectors $\mathbf{Q}_1 = (\pi, 0)$ and $\mathbf{Q}_2 = (0, \pi)$ (using single iron Brillouin zone notation). The relative orientations and amplitudes of the magnetic vector order parameters $\mathbf{M}_i$ allow three types of order [6], as illustrated in Fig. 1(c): (i) A single-$\mathbf{Q}$ SSDW, which takes place when only one of the $\mathbf{M}_i$ is nonzero. This is the phase observed in most iron pnictide parent compounds [46–48]. (ii) A collinear double-$\mathbf{Q}$ order dubbed charge-spin density-wave (CSDW), corresponding to $\mathbf{M}_1 = \pm\mathbf{M}_2$. This phase is realized, e.g., in Na-doped $SrFe_2As_2$ [13]. (iii) A coplanar double-$\mathbf{Q}$ order dubbed spin-vortex crystal (SVC), characterized by $\mathbf{M}_1 \perp \mathbf{M}_2$ and $|\mathbf{M}_1| = |\mathbf{M}_2|$. This phase is realized in Ni-doped $CaKFe_4As_4$ [11]. Although the three types of order share the same magnetic wave vectors, they break distinct symmetries of the lattice: the SSDW phase is orthorhombic whereas the CSDW and SVC phases are tetragonal [4,6,31].

To discuss the universal properties of the magnetic phase diagram, we introduce the magnetic action in terms of $\mathbf{M}_1$ and $\mathbf{M}_2$ [4,5,25,28]. In the spin-isotropic case, there are four terms allowed by tetragonal and time-reversal symmetries:

$$S = \int_k r_0(k)(\mathbf{M}_1^2 + \mathbf{M}_2^2) + \frac{u}{2}\int_r (\mathbf{M}_1^2 + \mathbf{M}_2^2)^2 - \frac{g}{2}\int_r (\mathbf{M}_1^2 - \mathbf{M}_2^2)^2 + 2w\int_r (\mathbf{M}_1 \cdot \mathbf{M}_2)^2. \quad (1)$$

The coefficient of the quadratic term, $r_0(k) = r_0 + \mathbf{k}^2 + \gamma|\omega_n|$, is the inverse bare susceptibility, with $r_0 \propto x - x_c$ denoting the distance to the mean-field QCP x_c. Here, $\mathbf{k}$ is the momentum, $\omega_n = 2\pi n T$ is the bosonic Matsubara frequency with temperature T, and γ is the Landau damping coefficient arising from the decay of magnetic excitations into particle-hole pairs. Note that $k = (i\omega_n, \mathbf{k})$ and $x = (\tau, \mathbf{r})$ with $\int_k \equiv T\sum_{\omega_n}\int d^2k/(2\pi)^2$ and $\int_r \equiv \int_0^{1/T} d\tau \int d^2r$. The quartic coefficient $u > 0$ penalizes strong amplitude fluctuations and ensures that the free energy is bounded. The quartic coefficient g favors either single-$\mathbf{Q}$ or double-$\mathbf{Q}$ configurations depending on whether it is positive or negative. Similarly, the quartic coefficient w favors collinear

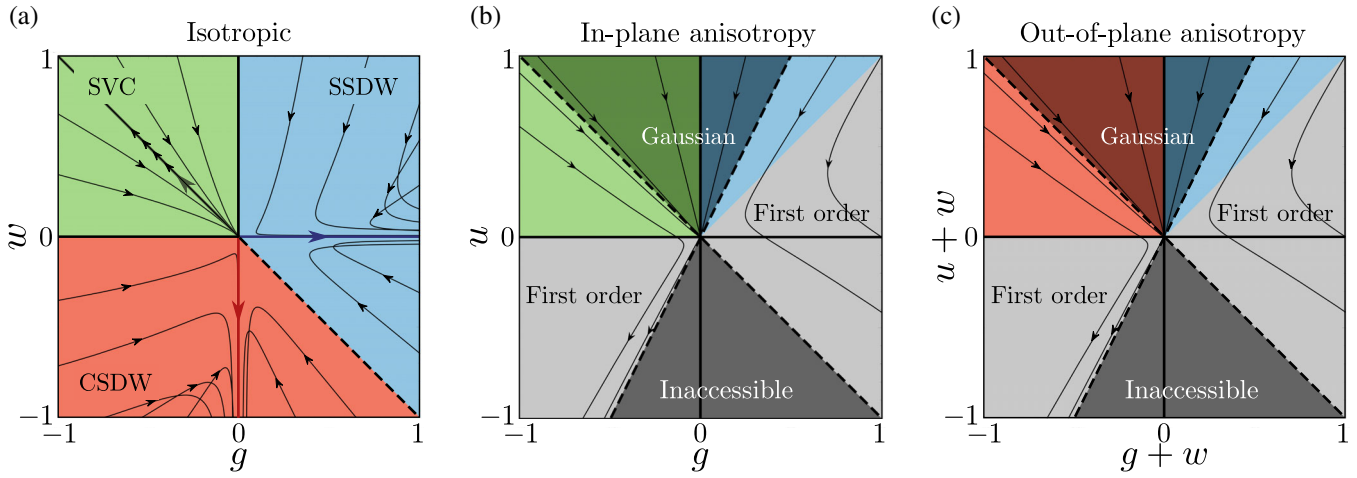

FIG. 2. (a) Mean-field magnetic phase diagram in the spin-isotropic case (colored background) and the RG flow lines for the zero-temperature, two-dimensional system. There are three fixed trajectories where the quartic coefficients diverge but their ratios remain finite. They are denoted by the thick darkly shaded lines, which lie deep inside each of the magnetic states. Because the flow lines are projections onto the $g - w$ plane, they appear to cross. (b)–(c) Flow diagrams for the cases of dominant (b) in-plane spin anisotropy ($\alpha_1 < \alpha_2, \alpha_3$ or $\alpha_2 < \alpha_1, \alpha_3$) and (c) out-of-plane spin anisotropy ($\alpha_3 < \alpha_1, \alpha_2$). Light gray areas denote regions in which the free energy is unbounded, corresponding to a first-order transition. The dark gray regions are inaccessible to any flow. Here, darker colors denote the regions attracted to the Gaussian fixed point, while lighter colors denote regions attracted to the fixed trajectories.

($w < 0$) or coplanar ($w > 0$) double-**Q** configurations. The mean-field phase diagram, obtained from straightforward minimization [4,32], is shown in Fig. 2(a).

Microscopic calculations are needed to obtain the coefficients for specific materials. Different approaches have been proposed, from first-principle to low-energy model calculations [4,5,25–31]. Several of them have found regimes in which, as a function of doping, the quartic coefficients change from favoring a C_2 (i.e., single-**Q**) phase to a C_4 (i.e., double-**Q**) phase, an effect essentially driven by changes in the band structure. Experimentally, however, the emergence of near-degenerate C_2-C_4 phases is observed for systems with rather different band structures, such as hole-doped $BaFe_2As_2$, electron-doped $CaKFe_4As_4$, and undoped pressurized FeSe. This suggests that the appearance of the C_4 phase may be associated with the universal properties of the action (1), and not only with material specific details.

To investigate this possibility, and go beyond the mean-field analysis of previous works, we take into account the effects of fluctuations via a renormalizaton-group (RG) calculation. In this approach, the microscopic results discussed above provide the starting point, which are the "bare" (i.e., mean-field) values of the quartic coefficients u_0, g_0, and w_0. Upon integrating out the high-energy magnetic fluctuations from the cutoff energy scale Λ to the energy E, these coefficients are renormalized, and become functions of the ratio Λ/E, often expressed in terms of the variable $\ell \equiv \ln[(\Lambda/E)]$. Near the putative magnetic QCP, the two-dimensional system is at its upper critical dimension, and we can use standard techniques [49] to derive the first-order differential RG flow equations for $u(\ell)$, $g(\ell)$, and $w(\ell)$. The goal is to find the fixed points that govern the critical behavior of these coefficients for a large number of different "initial conditions" u_0, g_0, and w_0, corresponding to different microscopic band structures.

The RG equations of Eq. (1) have been previously derived [50–53], but the fixed point analysis was generally restricted to the subspace of the SSDW phase. Our global analysis reveals that, for three-component vectors, no stable fixed points exist. Instead, the RG flow displays three fixed trajectories, in which the quartic coefficients diverge at $\ell = \ell_c$, but their ratios remain fixed. They are illustrated by the colored thick lines in Fig. 2(a): in all of them, $u(\ell \to \ell_c) \to -\infty$, but the ratios acquire different values. The blue fixed trajectory has $g(\ell_c)/u(\ell_c) = -1$ and $w(\ell_c)/g(\ell_c) = 0$, corresponding to a system deep inside the SSDW phase. The basin of attraction corresponds to the blue region of the mean-field phase diagram in Fig. 2(a), implying that fluctuations do not alter the nature of the mean-field ground state. Similarly, the two other fixed trajectories are the red line $w(\ell_c)/u(\ell_c) = 1$ and $g(\ell_c)/w(\ell_c) = 0$, corresponding to a system deep inside the CSDW phase, and the green line $g(\ell_c)/u(\ell_c) = 0$ and $g(\ell_c)/w(\ell_c) = -1$, corresponding to a system deep inside the SVC phase.

Thus, fluctuations move the system deep into one of the ordered phases, lifting any near degeneracy between the C_2 and C_4 phases obtained from microscopic models in the mean-field level. This makes it difficult to explain the proliferation of coexisting C_2 and C_4 phases near the different optimal-doped compounds. Furthermore, the action becomes unbounded at the fixed trajectories, indicating a first-order quantum phase transition, and thus no quantum critical fluctuations.

Renormalization group flow of the anisotropic case.—A crucial ingredient missing in the analysis above is the spin anisotropy that is generated by the spin-orbit coupling present in these systems [36,44,54]. Indeed, experimentally, the magnetic moments of each configuration are found to point to well-defined directions: in the SSDW phase, the moments point in-plane, parallel to the wave-vector direction [8]; in the SVC phase, the moments also point in-plane, making 45° with respect to the wave-vector directions [11]; in the CSDW phase, the moments point out-of-plane [13,16] [see Fig. 1(c)]. At the quadratic level, the spin-orbit coupling gives rise to three different spin-anisotropic terms [29,55]:

$$S^{(2)}_{\mathrm{SOC}} = \int_k r_0(k)(\mathbf{M}_1^2 + \mathbf{M}_2^2) + \alpha_1 \int_k (M_{x,1}^2 + M_{y,2}^2) + \alpha_2 \int_k (M_{x,2}^2 + M_{y,1}^2) + \alpha_3 \int_k (M_{z,1}^2 + M_{z,2}^2). \quad (2)$$

The physical interpretation of each term is apparent: a small α_1 favors in-plane moments parallel to the wave-vector directions; a small α_2 favors in-plane moments perpendicular to the wave-vector directions; and a small α_3 favors out-of-plane moments. While the SSDW supports any of these three magnetization directions, SVC is only compatible with the α_1 and α_2 terms, and CSDW only with the α_3 term. Thus, the presence of spin anisotropies makes it impossible for the three magnetic ground states to be nearly degenerate, but they do allow, in principle, for SSDW to be near degenerate with either CSDW or SVC.

Note that the anisotropy in the quadratic terms generates anisotropies in the quartic terms. While a full solution of the RG equations is presented in Ref. [56], here we focus on limiting cases that capture the main properties of the RG flow. Because of their scaling dimension, the quadratic coefficients $r_0 + \alpha_i$ can display two possible asymptotic behaviors as $\ell \to \ell_c$. Either $r_0 + \alpha_i \to \infty$, in which case the associated spin components are quenched and do not contribute to the action, or $r_0 + \alpha_i \to -\infty$, signaling a transition and the condensation of the spin components related to α_i. Importantly, the quadratic coefficient α_i with the smallest bare value selects which components will condense.

Let us first consider the case of dominant in-plane anisotropy, where initially $\alpha_1(\ell = 0) < \alpha_2(\ell = 0)$, $\alpha_3(\ell = 0)$. The possible ground states are the SSDW phase with moments pointing parallel to the ordering vectors and the (hedgehog)-SVC phase [11]; see Fig. 1(c). According to the discussion above, only the components associated with α_1 (namely, $M_{x,1}$ and $M_{y,2}$) will condense, while the others can be neglected. Hence, the universal properties of the action are the same as those of the action (1) restricted only to the $M_{x,1}$ and $M_{y,2}$ fields. As a consequence, w plays no role in this case. The RG flow of this action is shown in Fig. 2(b). Besides the two fixed trajectories equivalent to the SSDW and SVC fixed trajectories of Fig. 2(b), a new Gaussian fixed point $u_{\alpha_1}(\ell_c) = g_{\alpha_1}(\ell_c) = 0$ emerges. Interestingly, we find a wide range of parameters for which this Gaussian fixed point is attractive, indicated by the region enclosed by the dashed lines in Fig. 2(b). We note that the same phase diagram appears in the case $\alpha_2(0) < \alpha_1(0)$, $\alpha_3(0)$.

In the case of dominant out-of-plane anisotropy, $\alpha_3(0) < \alpha_1(0)$, $\alpha_2(0)$, the effective action has the same form as Eq. (1), but restricted only to the $M_{z,1}$ and $M_{z,2}$ fields. In this case, w cannot be ignored although its effect can be incorporated in a shift of u and g, as seen in the axes of Fig. 2(c). The possible ground states in this case are the SSDW and CSDW with out-of-plane moments. As shown in Fig. 2(c), the RG flow is analogous to the case of dominant in-plane anisotropy. It displays two fixed trajectories corresponding to the SSDW and CSDW states, and the Gaussian fixed point where the quartic coefficients vanish.

The main result of our analysis is the appearance of an attractive Gaussian fixed point in the RG flow of the anisotropic spin action. To understand its significance, we first note that it signals a second-order quantum phase transition (and thus quantum critical fluctuations), in contrast to the case of fixed trajectories, which signals first-order transitions. More importantly, at the Gaussian fixed point, the SSDW state is degenerate with one of the C_4 phases—either the SVC phase for dominant in-plane anisotropy or the CSDW phase for dominant out-of-plane anisotropy. This degeneracy is due to the fact that, when $g = w = 0$ in the action (1), the energies of the C_2 and C_4 magnetic ground states have the same value. The fact that the Gaussian fixed point has a wide basin of attraction implies that, even if the bare (mean-field) values of g and w are not near the phase boundary between the C_2 and the C_4 phases, quantum fluctuations will bring the system to this special point of the phase diagram.

Discussion.—Our results provide a compelling scenario to explain the experimentally observed proliferation of C_4 phases in close proximity to the C_2 symmetric SSDW phase as optimal doping is approached in different iron-based compounds [9–24]. Instead of attributing this behavior to band structure effects, which requires fine-tuning in a wide range of compounds, our approach reveals that the emergence of C_4 phases near the putative magnetic QCP is a universal property of the low-energy magnetic properties of these materials. It arises from the interplay between spin-orbit coupling and magnetic fluctuations. We emphasize that these results are not contradictory, but complementary to the microscopic calculations [4,5,25–31]. In fact, our results in tandem with the mean-field results of, e.g., Refs. [30,31] show that as long as the band structure effects bring the system closer, rather than farther from the degeneracy points, fluctuations will take over and move the system closer to the degeneracy point. Importantly, this effect is prominent near the putative magnetic QCP, when

the system is at its upper critical dimension. This sheds new light on why the proliferation of C_2 and C_4 phases takes place near optimal doping, where the magnetic transition temperature is suppressed to zero.

An important question is how this emergent C_2-C_4 near-degeneracy impacts superconductivity. Several works have proposed an s^{+-} state driven by fluctuations of the SSDW state [1–3]. Usually, the existence of additional channels of magnetic fluctuations does not guarantee an enhancement of T_c. On the contrary, in the case of ferromagnetic [57] or Néel fluctuations [58], they can cause pair breaking and promote competing superconducting states that suppress T_c of the s^{+-} state. In our case, however, fluctuations associated with the C_2 and C_4 phases are peaked at the same wave vectors $(\pi, 0)$ and $(0, \pi)$, and thus support the same pairing state. Therefore, one expects that this near degeneracy, by enhancing the phase space of fluctuations, may cause an enhancement of T_c.

The authors are grateful to W. R. Meier, A. E. Böhmer, J. Kang, A. Kreisel, M. N. Gastiasoro, D. D. Scherer, and M. Schütt for valuable discussions. M. H. C. and R. M. F. were supported by the U.S. Department of Energy, Office of Science, Basic Energy Sciences, under Award No. DE-SC0012336. B. M. A. acknowledges financial support from a Lundbeckfond fellowship (Grant No. A9318). P. P. O. acknowledges support from Iowa State University Startup Funds.

[1] P. J. Hirschfeld, M. M. Korshunov, and I. I. Mazin, Rep. Prog. Phys. **74**, 124508 (2011).
[2] A. V. Chubukov, Annu. Rev. Condens. Matter Phys. **3**, 57 (2012).
[3] D. J. Scalapino, Rev. Mod. Phys. **84**, 1383 (2012).
[4] J. Lorenzana, G. Seibold, C. Ortix, and M. Grilli, Phys. Rev. Lett. **101**, 186402 (2008).
[5] I. Eremin and A. V. Chubukov, Phys. Rev. B **81**, 024511 (2010).
[6] R. M. Fernandes, S. A. Kivelson, and E. Berg, Phys. Rev. B **93**, 014511 (2016).
[7] P. Dai, J. Hu, and E. Dagotto, Nat. Phys. **8**, 709 (2012).
[8] P. Dai, Rev. Mod. Phys. **87**, 855 (2015).
[9] M. G. Kim, A. Kreyssig, A. Thaler, D. K. Pratt, W. Tian, J. L. Zarestky, M. A. Green, S. L. Bud'ko, P. C. Canfield, R. J. McQueeney, and A. I. Goldman, Phys. Rev. B **82**, 220503(R) (2010).
[10] E. Hassinger, G. Gredat, F. Valade, S. R. de Cotret, A. Juneau-Fecteau, J.-P. Reid, H. Kim, M. A. Tanatar, R. Prozorov, B. Shen, H.-H. Wen, N. Doiron-Leyraud, and L. Taillefer, Phys. Rev. B **86**, 140502 (2012).
[11] W. R. Meier, Q.-P. Ding, A. Kreyssig, S. L. Bud'ko, A. Sapkota, K. Kothapalli, V. Borisov, R. Valenti, C. D. Batista, P. P. Orth, R. M. Fernandes, A. I. Goldman, Y. Furukawa, A. E. Böhmer, and P. C. Canfield, npj Quantum Materials **3**, 5 (2018).
[12] S. Avci, O. Chmaissem, J. M. Allred, S. Rosenkranz, I. Eremin, A. V. Chubukov, D. E. Bugaris, D. Y. Chung, M. G. Kanatzidis, J.-P Castellan, J. A. Schlueter, H. Claus, D. D. Khalyavin, P. Manuel, A. Daoud-Aladine, and R. Osborn, Nat. Commun. **5**, 3845 (2014).
[13] J. M. Allred, K. M. Taddei, D. E. Bugaris, M. J. Krogstad, S. H. Lapidus, D. Y. Chung, H. Claus, M. G. Kanatzidis, D. E. Brown, J. Kang, R. M. Fernandes, I. Eremin, S. Rosenkranz, O. Chmaissem, and R. Osborn, Nat. Phys. **12**, 493 (2016).
[14] A. E. Böhmer, F. Hardy, L. Wang, T. Wolf, P. Schweiss, and C. Meingast, Nat. Commun. **6**, 7911 (2015).
[15] L. Wang, F. Hardy, A. E. Böhmer, T. Wolf, P. Schweiss, and C. Meingast, Phys. Rev. B **93**, 014514 (2016).
[16] F. Waßer, A. Schneidewind, Y. Sidis, S. Wurmehl, S. Aswartham, B. Büchner, and M. Braden, Phys. Rev. B **91**, 060505(R) (2015).
[17] D. D. Khalyavin, S. W. Lovesey, P. Manuel, F. Krüger, S. Rosenkranz, J. M. Allred, O. Chmaissem, and R. Osborn, Phys. Rev. B **90**, 174511 (2014).
[18] B. P. P. Mallett, P. Marsik, M. Yazdi-Rizi, T. Wolf, A. E. Böhmer, F. Hardy, C. Meingast, D. Munzar, and C. Bernhard, Phys. Rev. Lett. **115**, 027003 (2015).
[19] Y. Zheng, P. M. Tam, J. Hou, A. E. Böhmer, T. Wolf, C. Meingast, and R. Lortz, Phys. Rev. B **93**, 104516 (2016).
[20] B. P. P. Mallett, Y. G. Pashkevich, A. Gusev, T. Wolf, and C. Bernhard, Europhys. Lett. **111**, 57001 (2015).
[21] K. M. Taddei, J. M. Allred, D. E. Bugaris, S. Lapidus, M. J. Krogstad, R. Stadel, H. Claus, D. Y. Chung, M. G. Kanatzidis, S. Rosenkranz, R. Osborn, and O. Chmaissem, Phys. Rev. B **93**, 134510 (2016).
[22] K. M. Taddei, J. M. Allred, D. E. Bugaris, S. H. Lapidus, M. J. Krogstad, H. Claus, D. Y. Chung, M. G. Kanatzidis, R. Osborn, S. Rosenkranz, and O. Chmaissem, Phys. Rev. B **95**, 064508 (2017).
[23] B. A. Frandsen, K. M. Taddei, M. Yi, A. Frano, Z. Guguchia, R. Yu, Q. Si, D. E. Bugaris, R. Stadel, R. Osborn, S. Rosenkranz, O. Chmaissem, and R. J. Birgeneau, Phys. Rev. Lett. **119**, 187001 (2017).
[24] E. Hassinger, G. Gredat, F. Valade, S. René de Cotret, O. Cyr-Choinière, A. Juneau-Fecteau, J.-Ph. Reid, H. Kim, M. A. Tanatar, R. Prozorov, B. Shen, H.-H. Wen, N. Doiron-Leyraud, and L. Taillefer, Phys. Rev. B **93**, 144401 (2016).
[25] G. Giovannetti, C. Ortix, M. Marsman, M. Capone, J. van den Brink, and J. Lorenzana, Nat. Commun. **2**, 398 (2011).
[26] P. M. R. Brydon, J. Schmiedt, and C. Timm, Phys. Rev. B **84**, 214510 (2011).
[27] J. Kang, X. Wang, A. V. Chubukov, and R. M. Fernandes, Phys. Rev. B **91**, 121104(R) (2015).
[28] X. Wang, J. Kang, and R. M. Fernandes, Phys. Rev. B **91**, 024401 (2015).
[29] M. H. Christensen, J. Kang, B. M. Andersen, I. Eremin, and R. M. Fernandes, Phys. Rev. B **92**, 214509 (2015).
[30] M. H. Christensen, D. D. Scherer, P. Kotetes, and B. M. Andersen, Phys. Rev. B **96**, 014523 (2017).
[31] M. N. Gastiasoro and B. M. Andersen, Phys. Rev. B **92**, 140506(R) (2015).
[32] X. Wang and R. M. Fernandes, Phys. Rev. B **89**, 144502 (2014).
[33] J. O'Halloran, D. F. Agterberg, M. X. Chen, and M. Weinert, Phys. Rev. B **95**, 075104 (2017).

[34] J. Wang, G.-Z. Liu, D. V. Efremov, and J. van den Brink, Phys. Rev. B **95**, 024511 (2017).
[35] M. Hoyer, R. M. Fernandes, A. Levchenko, and J. Schmalian, Phys. Rev. B **93**, 144414 (2016).
[36] S. V. Borisenko, D. V. Evtushinsky, Z.-H. Liu, I. Morozov, R. Kappenberger, S. Wurmehl, B. Büchner, A. N. Yaresko, T. K. Kim, M. Hoesch, T. Wolf, and N. D. Zhigadlo, Nat. Phys. **12**, 311 (2016).
[37] O. J. Lipscombe, L. W. Harriger, P. G. Freeman, M. Enderle, C. Zhang, M. Wang, T. Egami, J. Hu, T. Xiang, M. R. Norman, and P. Dai, Phys. Rev. B **82**, 064515 (2010).
[38] N. Qureshi, P. Steffens, S. Wurmehl, S. Aswartham, B. Büchner, and M. Braden, Phys. Rev. B **86**, 060410 (2012).
[39] C. Wang, R. Zhang, F. Wang, H. Luo, L. P. Regnault, P. Dai, and Y. Li, Phys. Rev. X **3**, 041036 (2013).
[40] Y. Song, L.-P. Regnault, C. Zhang, G. Tan, S. V. Carr, S. Chi, A. D. Christianson, T. Xiang, and P. Dai, Phys. Rev. B **88**, 134512 (2013).
[41] P. Steffens, C. H. Lee, N. Qureshi, K. Kihou, A. Iyo, H. Eisaki, and M. Braden, Phys. Rev. Lett. **110**, 137001 (2013).
[42] Z. Li, D. L. Sun, C. T. Lin, Y. H. Su, J. P. Hu, and G.-Q. Zheng, Phys. Rev. B **83**, 140506 (2011).
[43] M. Hirano, Y. Yamada, T. Saito, R. Nagashima, T. Konishi, T. Toriyama, Y. Ohta, H. Fukazawa, Y. Kohori, Y. Furukawa, K. Kihou, C.-H. Lee, A. Iyo, and H. Eisaki, J. Phys. Soc. Jpn. **81**, 054704 (2012).
[44] T. Kissikov, R. Sarkar, M. Lawson, B. T. Bush, E. I. Timmons, M. A. Tanatar, R. Prozorov, S. L. Bud'ko, P. C. Canfield, R. M. Fernandes, and N. J. Curro, Nat. Commun. **9**, 1058 (2018).
[45] A. E. Böhmer, K. Kothapalli, W. T. Jayasekara, J. M. Wilde, B. Li, A. Sapkota, B. G. Ueland, P. Das, Y. Xiao, W. Bi, J. Zhao, E. E. Alp, S. L. Bud'ko, P. C. Canfield, A. I. Goldman, and A. Kreyssig, arXiv:1803.09449.
[46] D. C. Johnston, Adv. Phys. **59**, 803 (2010).
[47] H. H. Wen and S. Li, Annu. Rev. Condens. Matter Phys. **2**, 121 (2011).
[48] J. Paglione and R. L. Greene, Nat. Phys. **6**, 645 (2010).
[49] K. G. Wilson and J. Kogut, Phys. Rep. **12**, 75 (1974).
[50] Y. Qi and C. Xu, Phys. Rev. B **80**, 094402 (2009).
[51] A. J. Millis, Phys. Rev. B **81**, 035117 (2010).
[52] Y. Kamiya, N. Kawashima, and C. D. Batista, Phys. Rev. B **84**, 214429 (2011).
[53] R. M. Fernandes, A. V. Chubukov, J. Knolle, I. Eremin, and J. Schmalian, Phys. Rev. B **85**, 024534 (2012).
[54] M. Ma, P. Bourges, Y. Sidis, Y. Xu, S. Li, B. Hu, J. Li, F. Wang, and Y. Li, Phys. Rev. X **7**, 021025 (2017).
[55] V. Cvetkovic and O. Vafek, Phys. Rev. B **88**, 134510 (2013).
[56] M. H. Christensen, P. P. Orth, B. M. Andersen, and R. M. Fernandes, companion paper, Phys. Rev. B, **98**, 014523 (2018).
[57] D. Guterding, H. O. Jeschke, I. I. Mazin, J. K. Glasbrenner, E. Bascones, and R. Valentí, Phys. Rev. Lett. **118**, 017204 (2017).
[58] R. M. Fernandes and A. J. Millis, Phys. Rev. Lett. **110**, 117004 (2013).